

Comparison of marine stratocumulus cloud top heights in the southeastern Pacific retrieved from satellites with coincident ship-based observations

Michael J. Garay,¹ Simon P. de Szoeke,² and Catherine M. Moroney³

Received 17 February 2008; revised 8 May 2008; accepted 11 June 2008; published 27 September 2008.

[1] In order to better understand the general problem of satellite cloud top height retrievals for low clouds, observations made by NOAA research vessels in the stratocumulus region in the southeastern Pacific during cruises in 2001 and 2003 to 2006 were matched with near-coincident retrievals from the Moderate Resolution Imaging Spectroradiometer (MODIS) and Multiangle Imaging SpectroRadiometer (MISR) instruments on the Terra satellite, along with a limited set of ISCCP 30-km (DX) retrievals. The ISCCP cloud top heights, determined from the cloud top pressures, were found to be biased high by between 1400 and 2000 m within the limited comparison data set. Like the International Satellite Cloud Climatology Project (ISCCP) results, the MODIS retrievals were biased high by more than 2000 m, while the MISR retrievals had errors on the order of 230 to 420 m, with the wind corrected heights having almost no bias. The extremely large bias in the ISCCP and MODIS retrievals was traced to their reliance on low-resolution observations or models of the atmospheric temperature structure. Cloud top height retrievals based on satellite cloud top temperatures and a constant atmospheric lapse rate agreed substantially better with the ship-based measurements.

Citation: Garay, M. J., S. P. de Szoeke, and C. M. Moroney (2008), Comparison of marine stratocumulus cloud top heights in the southeastern Pacific retrieved from satellites with coincident ship-based observations, *J. Geophys. Res.*, *113*, D18204, doi:10.1029/2008JD009975.

1. Introduction

[2] Studies based on satellite observations have shown that stratocumulus clouds common off the western coasts of continents produce the largest net radiative forcing to the climate system [e.g., Hartmann *et al.*, 1992]. However, correctly modeling these clouds in general circulation models (GCMs) remains a significant challenge. Biases in sea surface temperatures in coupled atmosphere-ocean GCMs, for example, have been traced to how stratocumulus clouds are simulated [e.g., Large and Danabasoglu, 2006; Mochizuki *et al.*, 2007], and low clouds have been identified as the primary cause of differences in GCM estimates of cloud feedback [e.g., Bony and Dufresne, 2005]. Moreover, comparisons between modeled stratocumulus cloud top heights and satellite retrievals from the International Satellite Cloud Climatology Project (ISCCP) [Rossow and Schiffer, 1999] suggest that either all GCMs place stratocumulus clouds too low in the atmosphere, or the ISCCP cloud tops

are biased high [e.g., Webb *et al.*, 2001; Zhang *et al.*, 2005; Schmidt *et al.*, 2006]. As an illustration of the magnitude of the discrepancy between the ISCCP and model results, Schmidt *et al.* [2006] found that the Goddard Institute for Space Studies (GISS) atmospheric GCM placed stratocumulus cloud tops at a mean altitude of approximately 1000 m. ISCCP reported cloud tops at approximately 2000 m, 1000 m higher than the model. This is significant because cloud top height is not only a fundamental parameter that affects both the surface and atmospheric radiation budgets [e.g., Stephens, 2005], but in marine stratocumulus regions the cloud top is also intimately associated with the depth of the atmospheric boundary layer [e.g., Bretherton *et al.*, 2004].

[3] Reasons for the difference between ISCCP and the models are not well understood [e.g., Zhang *et al.*, 2005]. Both Webb *et al.* [2001] and Schmidt *et al.* [2006] suggest that the problem may lie in the ISCCP cloud top height retrieval approach. Wang *et al.* [1999] found that between 450 and 660 m of the satellite retrieval error could be attributed to errors in the Television Infrared Observation Satellite (TIROS) Operational Vertical Sounder (TOVS) atmospheric temperature profiles used in the ISCCP algorithm as described by Rossow and Schiffer [1999]. Del Genio *et al.* [2005] considered TOVS biases, as well as undetected thin cirrus, as potential reasons for the observed discrepancy between ISCCP retrievals and atmospheric models.

¹Intelligence and Information Systems, Raytheon Corporation, Pasadena, California, USA.

²International Pacific Research Center, School of Ocean and Earth Science and Technology, University of Hawaii, Honolulu, Hawaii, USA.

³Jet Propulsion Laboratory, California Institute of Technology, Pasadena, California, USA.

[4] In this paper we address the broader issue of satellite retrievals of cloud top heights in marine stratocumulus regimes. Because of their prevalence away from land, detailed observations of marine stratocumulus cloud top heights from in situ measurements are infrequent. Here we take advantage of a set of multiyear stratocumulus observations compiled by the National Oceanic and Atmospheric Administration (NOAA) from cruises in the stratocumulus regime off the western coast of South America, beginning with the East Pacific Investigation of Climate (EPIC) field campaign in 2001 [Bretherton *et al.*, 2004]. These observations are compared with temporally and spatially coincident retrievals of cloud top height from ISCCP and the NASA EOS Terra satellite.

[5] ISCCP provides a nearly 25 year record of cloud and surface properties derived from observations made by instruments on operational weather satellites including the Advanced Very High Resolution Radiometer (AVHRR) on the NOAA polar orbiting platforms and the imagers on the Geostationary Operational Environmental Satellites (GOES) [Rossow and Schiffer, 1999]. Cloud top pressures are provided at up to 30 km horizontal resolution. Even higher horizontal resolution (5 km) cloud top retrievals are available from the Moderate Resolution Imaging Spectroradiometer (MODIS) on the Terra satellite, which has been operational since the year 2000 [Platnick *et al.*, 2003]. For marine stratocumulus clouds both ISCCP and MODIS rely on similar retrieval approaches that depend on observations or models of the atmospheric temperature structure. For comparison, we also consider retrievals of cloud top height provided at 1.1 km horizontal resolution from the Multiangle Imaging SpectroRadiometer (MISR) on the Terra satellite. MISR has the unique ability to retrieve both cloud top height and cloud motion vector winds simultaneously using a stereophotogrammetric technique, which is completely independent of ancillary information regarding the state of the atmosphere [Horváth and Davies, 2001a; Moroney *et al.*, 2002; Zong *et al.*, 2002].

2. Data

[6] In an effort to better understand the sparsely observed, but climatologically important, stratocumulus regime off the coast of South America, the EPIC field campaign took place in October 2001 [Bretherton *et al.*, 2004; Comstock *et al.*, 2005]. Additional cruises, some carried out under the NOAA Climate Variability and Predictability (CLIVAR) Pan American Climate Studies (PACS) program, took place in the region in October 2003, December 2004, October 2005, and October 2006 [Kollias *et al.*, 2004; Tomlinson *et al.*, 2007]. The tracks taken during these cruises are shown in Figure 1, along with the location of the Woods Hole Oceanographic Institute (WHOI) buoy, which provides the only continuous in situ data set in the region [Bretherton *et al.*, 2004]. Most cruises began to the north of the stratocumulus region (lighter portion of the tracks in Figure 1), approached the WHOI buoy, then headed toward the South American coast along 20°S latitude (darker portion of the tracks).

[7] The research vessels *Roger Revelle* and *Ronald H. Brown* were both used at different times for these cruises. The vessels were equipped with the seagoing NOAA

Environmental Technology Laboratory (ETL, now part of the NOAA Earth System Research Laboratory, ESRL) remote sensing suite of instruments [Fairall *et al.*, 1997]. Cloud top heights were determined using either returns from a vertically pointing 8.6-mm wavelength cloud radar, when available, or backscatter from a 915 MHz wind profiler. A comprehensive data set has been assembled from these cloud top height measurements, which were calibrated to match the observed height of the temperature inversion at the top of the boundary layer determined from coincident radiosonde launches. The vertical resolution of the cloud top heights in this data set is approximately 60 m, and the observations are averaged over a sampling period of 10 min. Radiosondes were launched from the ship at 3-h intervals during EPIC 2001 [Bretherton *et al.*, 2004] and less frequently in other years. Because the comprehensive data set provides better temporal and spatial coverage than the radiosonde launches themselves, the use of these data allow for direct comparison of nearly coincident retrievals of cloud top heights from both the ship-based and satellite instruments.

[8] The ISCCP project produces cloud data sets at a variety of temporal and spatial resolutions, which are described in detail by Rossow and Schiffer [1999]. The highest-resolution cloud product, known as DX data, has a horizontal resolution of 30 km and is available every 3 h. The DX data provide information on individual pixels from individual satellite instruments including calibrated radiances, information on satellite viewing geometry, results of the cloud detection algorithm, and retrievals of surface and cloud properties, such as cloud top temperature and pressure. The more commonly used 3-hourly D1 and monthly D2 data sets are derived from the DX data [Rossow and Schiffer, 1999]. For this study the DX data from the GOES-East and GOES-West operational satellites were used, which included GOES-8 and GOES-12 (East) and GOES-10 (West) over the time period of interest. The ISCCP processing first samples the temporal frequency of GOES observations to once every 3 h. Higher-resolution (1 km at nadir) visible channel data are then averaged to match the lower-resolution (4 km at nadir) infrared channels on the GOES imagers [Menzel and Purdom, 1994]. These data are then sampled to 30-km resolution for use in the next stage of the ISCCP processing. If the pixel radiance differs from the associated clear-sky radiance by more than a specific threshold, that pixel is labeled as cloudy [Rossow and Schiffer, 1999]. If a pixel is determined to be cloudy, then cloud top temperature is determined from the infrared radiance using the results of a radiative transfer model, including a correction for atmospheric water vapor. For clouds with a low visible optical thickness, a correction is also made in the cloud top temperature to account for the small amount of surface IR radiation that may pass through such a cloud, effectively reducing the cloud top temperature for some daytime observations [Rossow *et al.*, 1996]. ISCCP reports both the infrared (IR) and corrected infrared (VIS) cloud top temperatures. Finally, the cloud top pressures are determined from the cloud top temperatures by matching the cloud top temperatures to the atmospheric temperature-pressure profile from the operational TOVS product [Rossow and Schiffer, 1999]. The operational TOVS profiles are produced by the NOAA National Environmental Satellite, Data, and Information

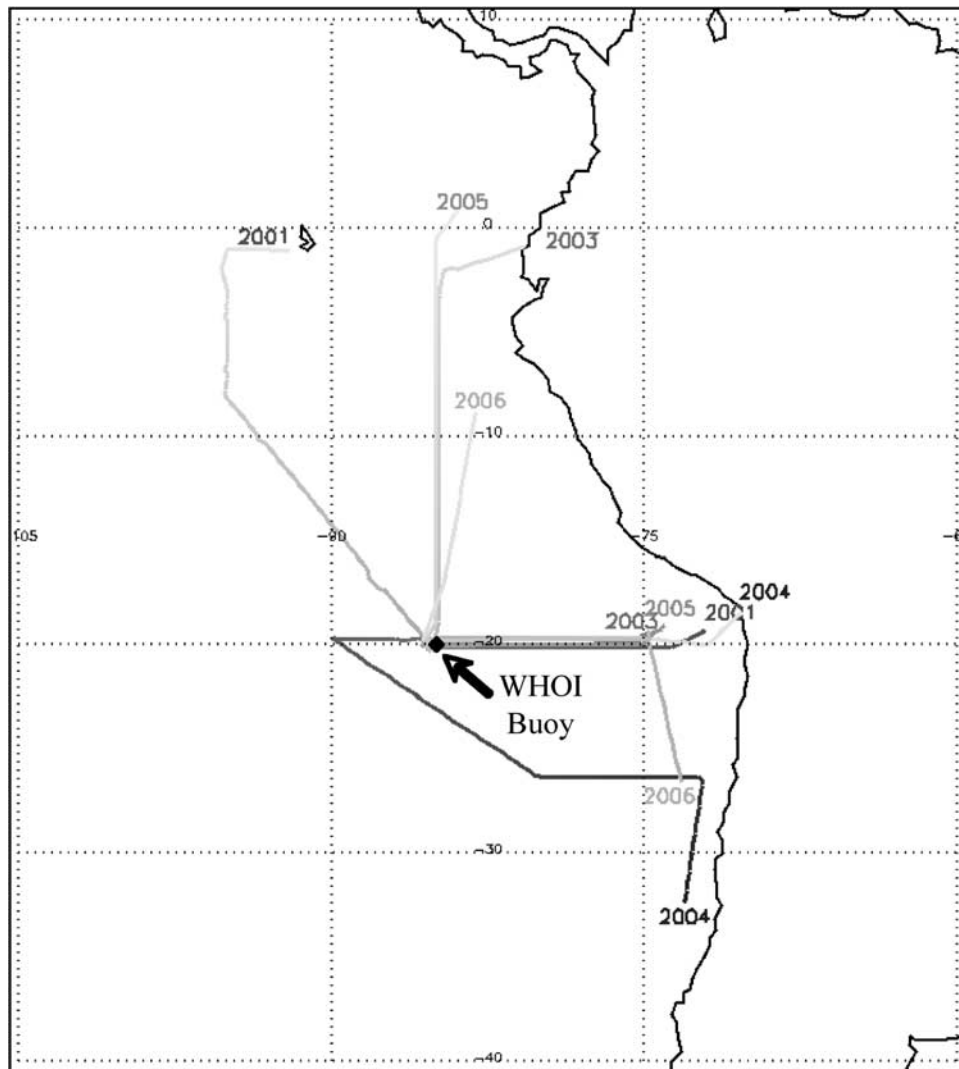


Figure 1. NOAA cruise tracks off the west coast of South America in 2001 and 2003–2006. The Woods Hole Oceanographic Institute (WHOI) buoy is indicated by the arrow. The shading of the tracks is lighter at the beginning of the cruise and becomes darker at the end of the track.

Service (NESDIS) at 2.5° spatial resolution once per day. If no TOVS information is available, a climatological atmospheric profile is used instead [Stubenrauch *et al.*, 1999].

[9] The MODIS cloud top heights used in this study were derived from the collection 5 level 2 (swath) MOD06 cloud properties product. An overview of this product can be found in Platnick *et al.* [2003]. The MODIS data are provided in five minute “granules” with a swath width of approximately 2330 km [King *et al.*, 2003]. Cloud top properties, including cloud top pressure and temperature, are reported at 5-km horizontal resolution. Changes to the product relevant to collection 5 are noted by Baum and Platnick [2006] and W. P. Menzel *et al.* (Cloud top properties and cloud phase algorithm theoretical basis document (MOD06CT/MYD06CT-ATBD-C005), 2006, available online at http://modis-atmos.gsfc.nasa.gov/_docs/MOD06CT:MYD06CT_ATBD_C005.pdf). For clouds with tops at altitudes less than about 3 km, such as stratocumulus clouds, cloud top pressures are determined using an IR retrieval. In this procedure cloud top temperatures are first

derived from the observed $11\ \mu\text{m}$ (band 31) brightness temperatures matched to radiative transfer model-derived temperatures assuming blackbody clouds. This is the same as the IR approach used by ISCCP. The cloud top temperature is then compared to the $1^\circ \times 1^\circ$ gridded meteorological temperature profile obtained every 6 h from the NCEP Global Data Assimilation System (GDAS) [Derber *et al.*, 1991] to yield a cloud top pressure. Because the $11\ \mu\text{m}$ brightness temperatures are retrieved at 1-km horizontal resolution, they must be aggregated to the 5-km resolution of the cloud top product. In collection 5 processing, this is done by aggregating the brightness temperatures only for those pixels determined to be cloudy by the MODIS cloud mask product (MOD35) [Ackerman *et al.*, 1998]; whereas in previous collections the brightness temperature was determined by aggregating all pixels within the 5 km region regardless of whether or not they contained cloud [e.g., Naud *et al.*, 2007]. For comparison with cloud top heights retrieved by MISR and the ship-based measurements, the operational cloud top pressures reported in the MOD06

product were converted to cloud top heights using the associated operational GDAS profile for the 1° grid box containing the MODIS observation. The GDAS pressures, along with the associated geopotential heights, were linearly interpolated from the standard 25 and 50 hPa pressure levels to 1 hPa levels. Differences between interpolating linearly or in the logarithm of the pressure are minor and do not affect the results. Since the pressures are monotonically decreasing, converting the cloud top pressures in this way yields unique cloud top (geopotential) heights. The ISCCP cloud top pressures, although derived from the TOVS profiles, were also converted to cloud top heights using the higher spatial and temporal resolution GDAS profile.

[10] The MISR cloud top heights used in this analysis were obtained from version F08_0017 of the standard level 2 (swath) top-of-atmosphere/cloud product (L2TC), which was the most current version of the operational processing algorithm at the time of this study. The effective width of the MISR instrument swath is approximately 380 km from the 705 km altitude of the Terra satellite [Diner *et al.*, 1998]. As described by Moroney *et al.* [2002], MISR retrieves cloud top heights using a stereophotogrammetric technique applied to pairs of MISR cameras. This approach requires sufficient contrast for an automatic pattern matching algorithm to identify common cloud elements [Muller *et al.*, 2002]. The use of integer precision in the pattern matching introduces an effective quantization in the heights of about 560 m in the vertical. While any single retrieval is affected by this quantization, statistically the error in the MISR retrievals is approximately ± 300 m [Moroney *et al.*, 2002; Naud *et al.*, 2004]. The L2TC product contains three fields, reported at 1.1-km horizontal resolution, used to produce the results described in this paper. The “StereoHeight_WithoutWinds” (no winds) field includes all retrieved stereo heights without any correction due to the motion produced by winds during the interval over which the scene is observed by MISR. The time difference between the first and last MISR camera view of a scene is approximately seven minutes, with less than a minute difference between observations from sequential cameras [Diner *et al.*, 1998]. Horváth and Davies [2001b] show that a 1 ms^{-1} wind along the direction of satellite motion (essentially north-south), where it has the largest effect, will result in a 70 to 80 m bias in the retrieved cloud top height. MISR also retrieves cloud motion vector winds on mesoscale domains at a resolution of 70.4 km. The retrieved winds, beginning with version F08_0016 of the software, have been shown to be an improvement over the winds produced using earlier versions [Davies *et al.*, 2007]. The “StereoHeight_BestWinds” (best winds) product contains the 1.1 km retrieved heights corrected using the 70.4 km MISR cloud motion vector winds that pass a variety of quality tests. The best winds heights are expected to represent the most accurate retrieval of the actual cloud top heights. The coverage of the best winds retrievals is lower than for the no winds retrievals, so when best winds heights are not available the “PrelimERStereoHeight_RawWinds” (raw winds) field is used instead. The raw winds represent heights corrected using all the available wind vectors, regardless of the quality of the winds. Together, the best winds and raw winds retrievals make up the “wind-corrected” heights reported in this paper. This follows the approach used by

Genkova *et al.* [2007] in studying trade cumulus cloud top heights.

[11] The tracks of the NOAA cruises shown in Figure 1 were compared with the Terra satellite overpasses for the appropriate dates to determine potential coincidences. Requiring the time difference between satellite and ship observations to be less than five minutes, and the ship observations to lie within the MISR swath, resulted in the selection of eight cases. This set represents the closest possible matches between the satellite and ship-based observations, where the potential effects of temporal and spatial inhomogeneity are minimized. Data from these same dates were also used for the comparison with the ISCCP DX retrievals from the GOES satellites. Although ISCCP provides a potentially much larger comparison set, requiring coincidence with the dates of the Terra observations facilitates intercomparisons with the higher-resolution data from MODIS and MISR. However, because of the overpass time of Terra falling between the 3-hourly ISCCP retrievals, there are no directly coincident Terra-ISCCP cases.

3. Results

3.1. Stratocumulus Cloud Top Heights From Cloud Top Pressures

[12] Figures 2a–2c show the cloud top heights determined from the reported cloud top pressures for ISCCP and MODIS plotted against the coincident reports of cloud top height from the ship-based instruments. One-to-one lines are included as aids to the eye. The ISCCP heights are for the 30-km pixel center closest to the location of the ship, while the MODIS heights are for the MODIS 5-km pixel containing the location of the ship. Symbols indicate the retrieval type and the satellite. To aid in interpretation, the GOES-East VIS retrievals are shifted by +50 m along the one-to-one line, the GOES-West IR retrievals are shifted by -50 m along the line, and the GOES-West VIS retrievals are shifted by -100 m along the line.

[13] A significant high bias is immediately evident in all three plots. The ISCCP retrievals from 1500:00 UT (Figure 2a) appear to agree better with the ship-based measurements, with the agreement becoming worse for the 1800:00 UT (Figure 2b) retrievals. The MODIS cloud top heights (Figure 2c) show the greatest bias, with a single low outlier with a cloud top just below 1000 m.

[14] A statistical analysis of the satellite retrievals of cloud top heights from cloud top pressures is provided in Table 1. The analysis is broken up by the time of retrieval, instrument, and retrieval algorithm. Mean cloud top heights are given for seven ISCCP cases at 1500:00 UT. Excluding a clear and a potentially cirrus contaminated case, determined from the cloud top retrievals themselves, leaves five ISCCP cases at 1800:00 UT. Note that at 1800:00 UT, the GOES-East IR and VIS retrievals were identical in these remaining cases, so they are combined in Table 1. A potentially cirrus contaminated case was similarly excluded for MODIS, based on visual inspection of the images and the reported cloud top height and phase, leaving seven cases coincident with the Terra satellite. While such small samples are not statistically significant, they indicate the approximate behavior of the retrievals in the region, since the

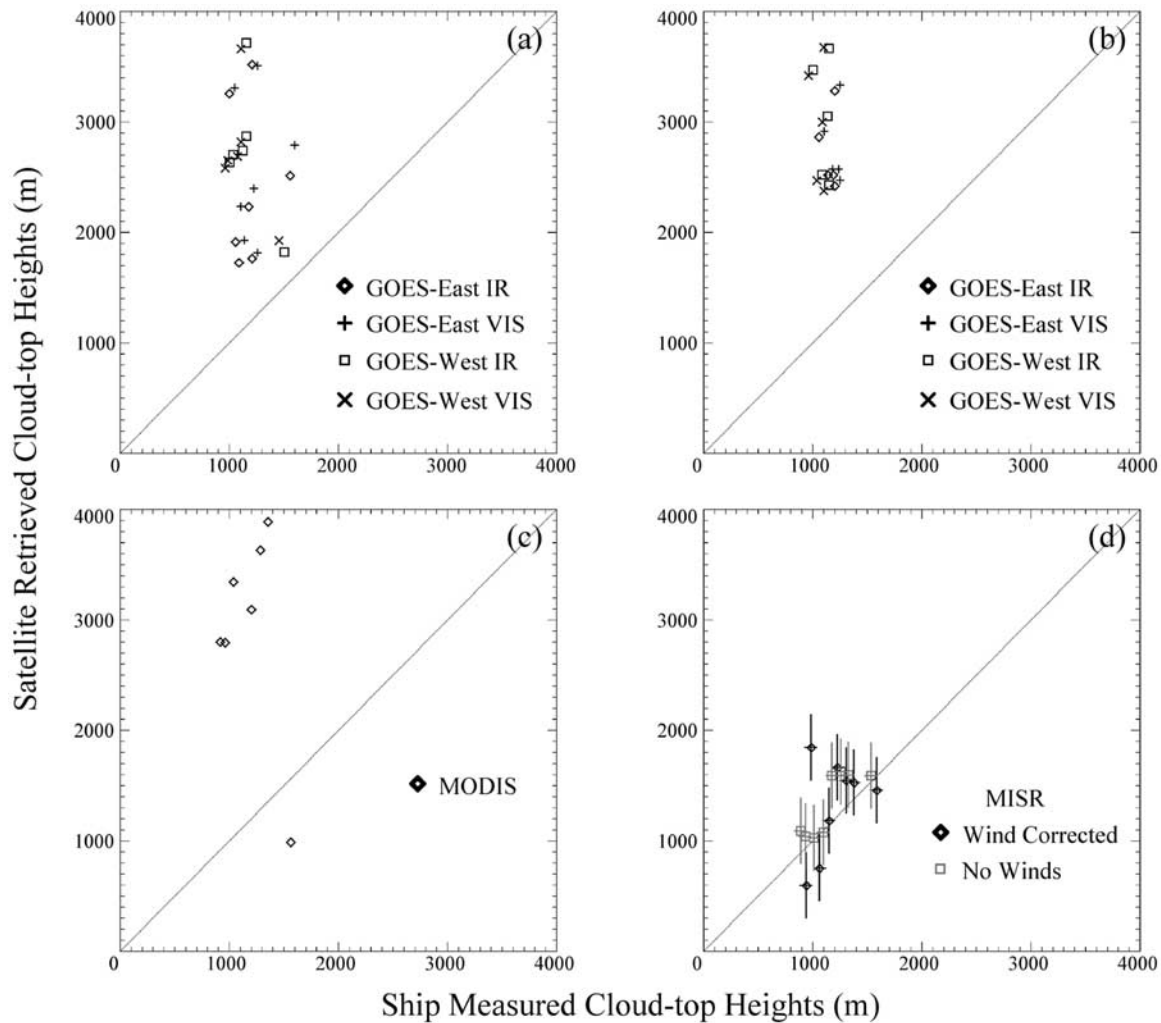


Figure 2. Comparison of cloud top heights from satellite retrievals and ship-based measurements in the marine stratocumulus region off the western coast of South America. (a) ISCCP DX cloud top heights determined from cloud top pressures retrieved from GOES-East and GOES-West at 15:00 UT. GOES-East retrievals made assuming blackbody (IR) clouds are shown as diamonds, GOES-West IR retrievals are shown as squares. Retrievals employing a visible channel correction (VIS) are indicated by pluses for GOES-East and crosses for GOES-West. Retrievals from each instrument are shifted slightly as an aid to interpretation. A one-to-one line is included for comparison. (b) Same as Figure 2a but for 18:00 UT retrievals. (c) MODIS retrievals of cloud top height derived from cloud top pressures. (d) MISR stereo height retrievals coincident with the MODIS retrievals. Wind-corrected heights are shown as black diamonds, and no winds heights are shown as gray squares. Error bars of ± 300 m are shown for the MISR retrievals and ± 60 m for the ship-based measurements. Points are shifted slightly as an aid to interpretation.

coincidence of overpasses with ship observations is essentially random with respect to the intrinsic variability of the clouds.

[15] The data in Table 1 show that the mean cloud top height in the stratocumulus region off the western coast of South America is around 1180 m, according to the ship-based measurements. There is some variability in these samples, on the order of 200 m. Satellite retrievals of the cloud top height, in contrast, range from 2400 m to about 3000 m, with correspondingly greater variability. Taking MODIS as an example, the cloud top heights have a mean of 2937 m. The mean cloud top pressure reported by MODIS is 720 hPa, which compares favorably with the

cloud top pressures shown by *Platnick et al.* [2003, Figure 3a] for the same stratocumulus region on 18 July 2001. On the basis of their color scale, it appears the cloud top pressures were also around 720 hPa on this date.

[16] Because the small sample sizes limit the utility of more powerful statistical approaches, we focus on two simple metrics to evaluate the agreement between the ship observations and satellite retrievals. The root mean squared error (RMSE) is used to assess the how two measurements x_1 and x_2 compare to one another over n samples. The Pearson product-moment correlation coefficient, or sample correlation coefficient, r , is the ratio of the covariance of the observations to the product of their standard deviations. A

Table 1. Statistical Comparison of Cloud Top Height Retrievals From Cloud Top Pressure and Associated Ship-Based Measurements

Observation	Mean (m)	σ (m)	RMS Error (m)	Correlation Coefficient r
Ship 1500 UT ($n = 7$)	1185	181		
GOES-East IR	2417	721	1409	0.03
GOES-East VIS	2516	658	1468	0.08
GOES-West IR	2987	750	1978	-0.67
GOES-West VIS	3009	714	1982	-0.63
Ship 1800 UT ($n = 5$)	1157	61		
GOES-East IR/VIS	2721	357	1597	-0.06
GOES-West IR	3075	553	1985	-0.23
GOES-West VIS	3087	571	2000	-0.21
Ship-Terra ($n = 7$)	1189	232		
MODIS	2937	950	2004	-0.37

perfect positive linear correlation is expressed by $r = 1$, and a perfect negative linear correlation is expressed by $r = -1$. One advantage of this metric is that squaring its value yields the coefficient of determination (R^2), which indicates the fraction of the variability in x_2 accounted for by a linear fit of x_1 to x_2 .

[17] As shown in Table 1, the RMSE ranges from 1409 m for the ISCCP IR retrievals at 1500:00 UT to 2004 m for the MODIS retrievals. The RMSE is larger for the GOES-West retrievals than the GOES-East retrievals. These mean differences are somewhat larger than the 960 m bias in the ISCCP cloud top heights relative to GCM modeled low clouds reported by *Schmidt et al.* [2006]. However, their results

represent a global annual average difference in low clouds, rather than a limited regional comparison as presented here. These results show that, even in the best case, these satellite retrievals of cloud top height are higher than the coincident ship-based heights by more than a factor of two.

[18] The correlation coefficient between the satellite-derived cloud top heights and the ship-based measurements indicate that the results are essentially uncorrelated, except for the GOES-West retrievals from 1500:00 UT, which show some anticorrelation. The maximum value of R^2 in for these retrievals is only 0.45 for the IR retrievals, explaining only 45% of the variance in the ship-based measurements. However, in this case, when the ship-based measurements decrease, the associated ISCCP heights increase, and vice versa. Of course, a much larger sample size would be required to establish the statistical significance of any of the results shown in Table 1. Even so, the magnitude of the differences is too large and consistent to be statistically fortuitous. Potential reasons for these results will be explored in the discussion section below.

3.2. Stereo-Derived Cloud Top Heights

[19] Figure 2d shows the plot of the MISR retrievals against the coincident ship measurements. The MISR wind-corrected heights are shown as black diamonds, with vertical error bars of ± 300 m, consistent with the expected error from all sources in the MISR measurements [e.g., *Moroney et al.*, 2002; *Naud et al.*, 2004]. The horizontal error bars show the ± 60 m uncertainty in the NOAA

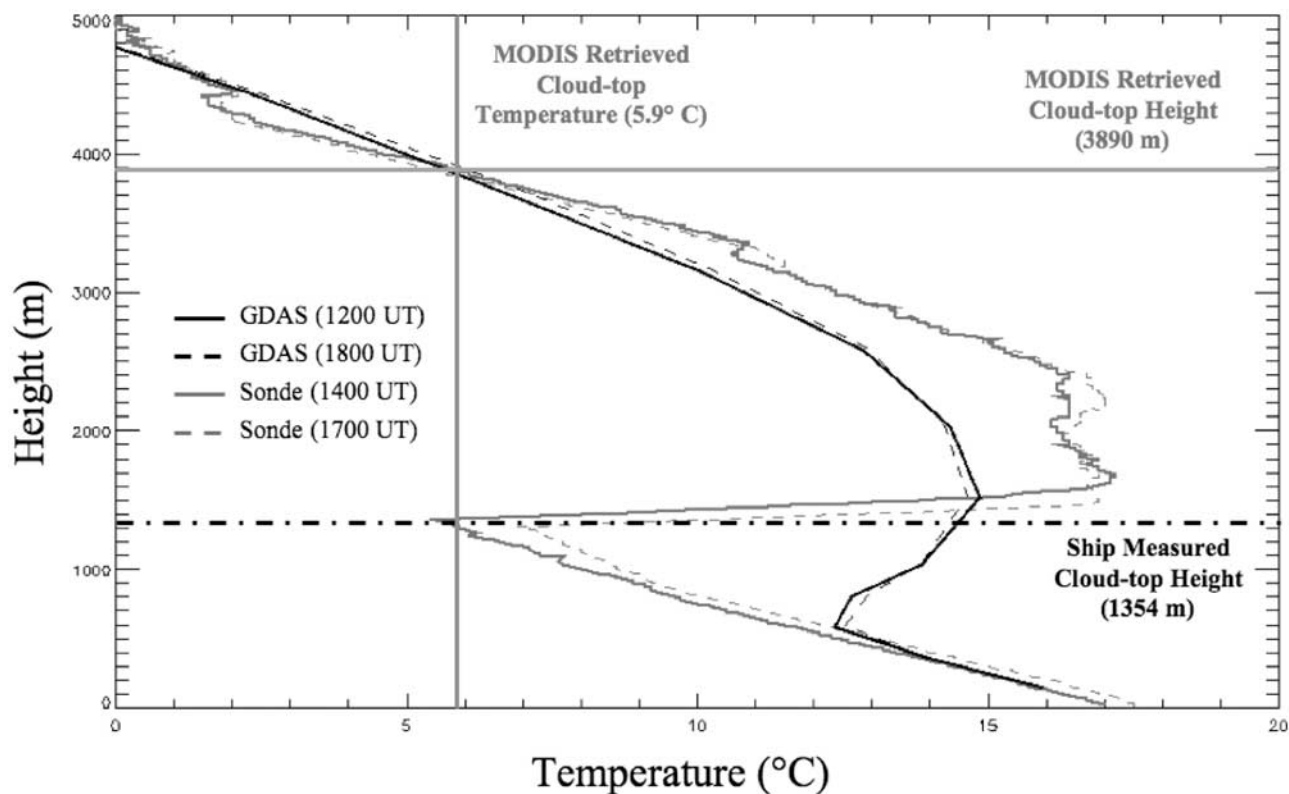


Figure 3. Comparison of GDAS (black) and radiosonde (gray) temperature retrievals below 5 km near the WHOI buoy on 16 October 2001. The dot-dashed line indicates the cloud top height reported by the ship-based measurement. The vertical gray line shows the operationally retrieved MODIS cloud top temperature. The horizontal gray line shows the resulting retrieved MODIS cloud top height.

Table 2. Statistical Comparison of MISR Stereo-Derived Cloud Top Height Retrievals and Associated Ship-Based Measurements

Observation	Mean (m)	σ (m)	RMS Error (m)	Correlation Coefficient r
All observations (n = 8)				
Ship	1181	216		
Wind corrected	1294	443	393	0.42
No winds	1352	289	229	0.83
Excluding outlier (n = 7)				
Ship	1212	213		
Wind corrected	1219	420	268	0.77
No winds	1394	286	242	0.79
MODIS coincident (n = 7)				
Ship	1189	232		
Wind corrected	1314	474	420	0.41
No winds	1388	292	245	0.85
MODIS	2937	950	2004	-0.37

measurements. The lighter squares show the MISR no winds heights and NOAA retrievals, along with the associated error bars. Note that the MISR wind-corrected heights have been shifted by +25 m along the one-to-one line, and the no winds heights have been shifted by -25 m along the line, as an aid to visualization.

[20] In contrast to the cloud top heights derived from cloud top pressures, the MISR retrievals are in very good agreement with the ship-based measurements, regardless of the application of a wind correction. Careful inspection of Figure 2d shows that the MISR no winds heights appear to have a slight positive bias relative to the ship measurements. The wind-corrected heights do not show this bias, at least in this limited data set. The clear outlier in the wind-corrected heights is from a case where MISR retrieved a cloud motion vector wind of 10.8 ms^{-1} , compared to the 6.9 ms^{-1} wind speed measured by the ship. As explained in section 2, the MISR wind correction is applied to all cloud top height retrievals within a mesoscale domain of 70.4 km. The winds within this domain may exhibit significant variability that is not represented on this scale. A more complete comparison of the MISR winds with surface wind measurements made onboard the NOAA research vessels will be the subject of a future study.

[21] Statistical summaries for the MISR retrievals are presented in Table 2. Results from all eight cases with valid height retrievals are listed in Table 2 for the ship and MISR retrievals. Excluding the outlier in the wind-corrected heights leaves the seven cases listed in Table 2. Excluding only the potentially cirrus contaminated case leaves the seven cases for which there are valid MODIS and MISR retrievals, which are listed in Table 2, with the MODIS values from Table 1 being included for comparison. Because of the impact of the outlier on the results, in the following, we only focus only on the set excluding the outlier ($n = 7$) in Table 2.

[22] Mean cloud top heights determined by the full complement of ship measurements coincident with Terra are around 1180 m, consistent with the results reported in Table 1 for the 1500:00 UT retrievals matched to ISCCP. Terra overpass times ranged from 1511:14 UT to 1618:27 UT within the coincident data set, suggesting closer agreement with the 1500:00 UT retrievals would be expected. The MISR wind-corrected heights have a mean around 1220 m, and the

no winds heights are around 1390 m, with the wind-corrected heights having a much larger standard deviation.

[23] The RMSE for the wind-corrected heights is 268 m, compared to 242 m for the no winds heights. The smaller RMSE coupled with a larger mean difference for the no winds heights is due to the fact that, on a case-by-case basis, the agreement between the no wind heights and the ship measurements is better than for the wind-corrected heights. This result shows the importance of applying matching criteria before calculating the difference in this type of comparison.

[24] Unlike the IR retrievals reported in Table 1, the correlation coefficients are 0.77 and 0.79 for the wind-corrected and no winds heights, respectively, for all seven coincident cases excluding the outlier. Both Table 2 and Figure 2d show quite clearly that the agreement between the ship-based measurements of cloud top height and MISR retrievals is very good. The application of a wind correction appears to reduce some bias in the no winds heights, consistent with the results of *Genkova et al.* [2007].

[25] However, the quantization of the MISR cloud top height retrievals requires consideration when interpreting the relative performance of the two MISR cloud top height retrieval approaches. The error bars in Figure 2d are ± 300 m, consistent with the size of the accumulated errors in the MISR retrievals [e.g., *Moroney et al.*, 2002; *Naud et al.*, 2004]. Evaluating the MISR retrievals relative to the height quantization by dividing the heights into increments of 560 m yields an alternate picture of the relative performance of the MISR algorithms. In this case, the MISR wind-corrected heights appear in the same height bin as the ship-based cloud top height measurements in all seven cases excluding the wind-corrected outlier. The no winds heights also appear in the same bin as the NOAA heights in seven of the eight total cases. The outlier was for a case where the cloud top height reported by the ship was almost exactly an integer multiple of 560 m. Consequently, the retrieved MISR cloud top height bins alternated between two values. In this case, the value reported for the no winds cloud top height was biased low relative to the ship-based measurement by one height bin. In general, considering the MISR cloud top heights in this manner shows that both the MISR no winds and wind-corrected heights agree with the NOAA observed heights within the performance characteristics of the operational MISR algorithms.

4. Discussion

4.1. Cloud Top Heights From Cloud Top Pressures

[26] In section 3.1, cloud top heights were derived from the cloud top pressures reported by ISCCP and MODIS and compared with coincident retrievals from ship-based instruments in the marine stratocumulus region off the western coast of South America. These comparisons are summarized in Figures 2a–2c and Table 1. Overall, these comparisons demonstrate that the cloud top heights determined using this approach are biased high by significantly more than 1000 m relative to the ship-based measurements. The MODIS cloud top algorithm team has recognized that a problem exists with the IR retrieval in situations dominated by strong inversions, such as the marine stratocumulus regions, for a number of years. The matching of the retrieved cloud top

temperature to the lower-resolution GDAS temperature profiles to derive cloud top pressure has been identified as the cause for this discrepancy (R. Frey, personal communication, 2007). To investigate this, we consider in greater detail the performance of the MODIS algorithm in the study region. Since ISCCP utilizes a similar algorithm, this analysis extends to those retrievals as well.

[27] In Figure 3 the temperature profiles from radiosondes launched at 1400:00 UT and 1700:00 UT on 16 October 2001 during the EPIC 2001 campaign are plotted against the temperature profiles at 1200:00 UT and 1800:00 UT from the GDAS 1° grid boxes containing the radiosonde launch locations. Note that neither radiosonde launch was coincident with the Terra satellite overpass, which occurred at 1607:05 UT on this date. The profile from 1400:00 UT is shown as the solid gray line, and the profile from 1700:00 UT is shown as the dashed gray line. Notice that the 14:00:00 UT profile reaches a minimum temperature around 5.5°C near the cloud top height of 1354 m, shown as the dash-dotted line, which was measured by the ship at 1604:59 UT. This indicates that the 1400:00 UT sounding is more representative of the region sampled during the Terra overpass since the cloud top is expected at the coldest point in the profile [e.g., *Bretherton et al.*, 2004]. The temperature jump just above this height is on the order of $+12^\circ\text{C}$, which is fairly typical of the region based on inspection of other radiosonde profiles.

[28] The GDAS temperature profiles for this date, shown in solid black for 1200:00 UT and dashed for 1800:00 UT, reveal little change over the 6-h period. The model is unable to correctly capture the local minimum temperature observed in the sounding, the altitude of this local minimum, or the altitude and temperature jump at the inversion. The local minimum temperature reported in the model is about 12.5°C , a bias of $+7^\circ\text{C}$ relative to the 1400:00 UT radiosonde profile. The altitude of this minimum temperature layer is only 600 m, compared to the 1354 m cloud top observed by the NOAA instruments. Finally, the temperature jump is only about $+2.5^\circ\text{C}$, compared to $+12^\circ\text{C}$ observed by the radiosonde.

[29] The effect these model biases have on the MODIS retrieval is illustrated by the gray vertical and horizontal lines in Figure 3. The vertical line shows the MODIS retrieved cloud top temperature of 5.9°C reported in the MOD06 product. The intersection of this temperature with the radiosonde profile agrees extremely well with the temperature at the base of the inversion, which also corresponds to the cloud top measured by the ship. The vertical line intersects all four profiles again at a much higher altitude. The horizontal gray line shows the retrieved MODIS cloud top height of 3890 m. Note that this horizontal line intersects the vertical temperature line at the same point as it intersects the temperature profiles. Because the MODIS IR algorithm relies on the GDAS profile (from 1200:00 UT, in this case), this is the only model height consistent with the observed cloud top temperature. The height is then converted to the reported cloud top pressure of 640 hPa. The behavior in this case is typical of most cases in the coincident data set.

[30] A contrasting situation is illustrated in Figure 4, from 14 October 2006. The radiosonde profile from 1500:00 UT is shown as the solid gray line, along with the GDAS

profiles from 1200:00 UT in solid black, and 1800:00 UT in long dashes. The Terra overpass was at 1554:58 UT, about an hour after the radiosonde launch. This time the GDAS model was able to better capture the structure of the temperature inversion, indicating a minimum temperature around 9°C just above 1000 m. The radiosonde profile shows the base of the inversion to be around 1300 m, with a temperature around 8.5°C . The cloud top temperature retrieved by MODIS was 9.3°C , slightly warmer than the radiosonde temperature at the base of the inversion, while the ship measured a cloud top height of 1561 m, shown as the dot-dashed line. These differences are most likely due to the time and space difference between the radiosonde launch and the coincident ship-satellite observations. Inspection of the MODIS imagery for this case showed that the ship was entering a region of broken cloudiness, so such variability is not unexpected.

[31] The MODIS cloud top retrieval algorithm for the MOD06 product determines the IR cloud top height by testing the GDAS model temperature at each altitude level in the model beginning with the tropopause and moving down to the surface. If the model temperature is less than the IR brightness temperature, then that level is stored, and the algorithm proceeds downward. If the temperature monotonically increases with decreasing height, this approach will identify the lowest altitude in the model with a temperature lower than the observed IR brightness temperature as the cloud top. If the temperature structure does not decrease monotonically (e.g., Figures 3 and 4), then the algorithm will still identify the lowest altitude in the GDAS model with a temperature lower than the IR brightness temperature. This is illustrated in Figure 4 where the retrieved cloud top height is 985 m. Had the algorithm selected the highest altitude in the GDAS model, then the cloud top would have been found at about 3050 m. The 14 October 2006 case is the only case in the coincident data set where the cloud top height derived from the reported MODIS cloud top pressure was lower than the ship-based measurement. In this situation, the GDAS model placed the altitude of the temperature inversion too low, so the MODIS retrieval was biased low as well. Given the vertical resolution of the model, it is not clear that the retrieval could have performed any better in this situation.

[32] These two cases illustrate the situation in the marine stratocumulus region off the west coast of South America. In most cases, the GDAS model was unable to adequately capture the structure and strength of the persistent temperature inversion. In fact, in one case (24 October 2001), the model had no inversion at all, although the radiosonde showed a temperature jump of $+14^\circ\text{C}$. When the inversion is modeled inadequately, the MODIS algorithm finds a matching cloud top temperature much higher in the atmosphere, leading to a large bias relative to the coincident ship-based measurements. Even if the GDAS model captures the structure of the inversion, deficiencies in the vertical model resolution can lead to other biases as illustrated by the 14 October 2006 case. This analysis shows that it is the reliance on the GDAS model temperature profile that lies at the heart of the infrared retrieval algorithm's difficulty in accurately retrieving cloud top heights, at least in the stratocumulus regime off the coast of South America. Although not shown here, the ISCCP retrievals have similar

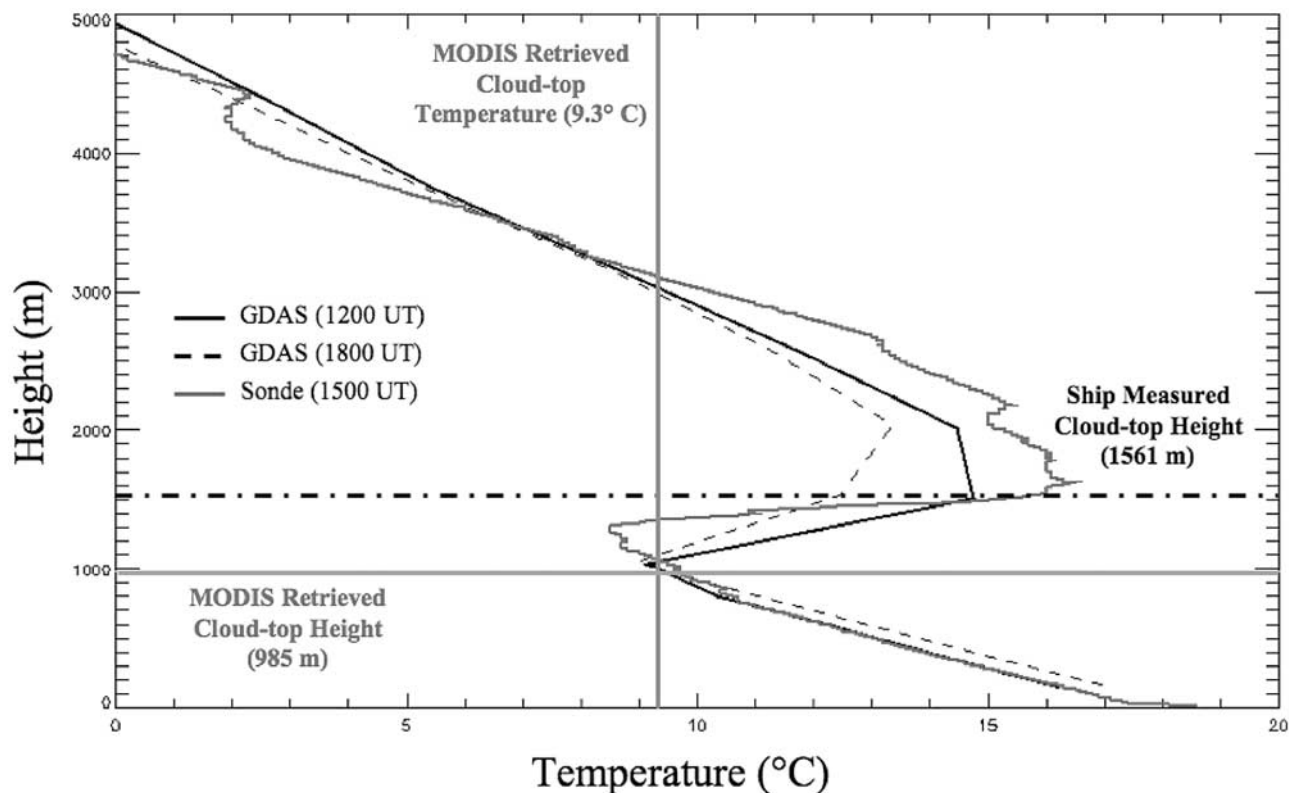


Figure 4. Same as Figure 3 but for 14 October 2006.

difficulties since the atmospheric temperature profile from TOVS has even lower spatial and temporal resolution than the GDAS model used by MODIS.

4.2. Constant Lapse Rate Retrievals of Stratocumulus Cloud Top Heights

[33] Given the issues with the retrieval of cloud top pressure described above, we consider an alternative method for determining the cloud top height for marine stratocumulus clouds. A simple approach, going back to the earliest weather satellites [e.g., *Fritz and Winston, 1962*], uses the difference between the IR cloud top and surface temperatures along with a standard lapse rate, Γ , to retrieve the cloud top height. The ISCCP code to read the D2 cloud product (D2READ, available online at <http://isccp.giss.nasa.gov/products/software.html>) calculates the cloud top height from the cloud top and surface temperature using a constant lapse rate of $6.5^{\circ}\text{C km}^{-1}$. Another common lapse rate used to calculate cloud top heights in marine stratocumulus regions is $7.1^{\circ}\text{C km}^{-1}$, derived by *Minnis et al. [1992]* from Electra aircraft soundings made off the coast of California during the First ISCCP Regional Experiment (FIRE).

[34] Plots of cloud top heights determined from the ISCCP data using these two lapse rates are shown in Figure 5a and 5b for 1500:00 UT and 1800:00 UT, respectively. Figure 5a does not show particularly good agreement between the ISCCP and ship-based cloud top heights. However, comparison with Figure 2a (note change in scale) indicates that the constant lapse rate produces cloud top heights in substantially better agreement with the ship-based

measurements. At 1800:00 UT, however, the spread in the retrieved cloud top heights is reduced relative to 1500:00 UT regardless of which lapse rate is applied.

[35] Table 3 shows the statistical comparisons between the ISCCP cloud top heights derived using a constant lapse rate and the ship-based measurements. The IR cloud top heights from Table 1 are included for comparison. In all cases, use of the constant lapse rate approach yields significantly lower cloud top heights than those found from the cloud top pressures. However, the standard deviation of the retrievals remains about the same, indicating that the variance is due to differences in the observed cloud top temperature, which affects both retrieval methods in a similar manner. With the reduction in the mean cloud top height, the RMSE also decreases significantly — by nearly a factor of six in the case of GOES-West at 1800:00 UT. However, the correlation coefficient does not show any particular improvement, which is due, once again, to the dependence of the results on the retrieval of cloud top temperature. Table 3 also indicates that the lapse rate of $7.1^{\circ}\text{C km}^{-1}$ yields slightly better results than $6.5^{\circ}\text{C km}^{-1}$, but differences in the results are not significant due to the small sample size.

[36] The higher-resolution MODIS data, which are easier to collocate with the ship than the ISCCP data, provide the unique opportunity to calculate the effective atmospheric lapse rate for each of the coincident cases. The NOAA instrumentation on the ship measures sea surface temperature (SST) at a depth of about 5 cm with a precision thermistor [*Fairall et al., 1997*]. These measurements are compared with the MODIS surface temperature measure-

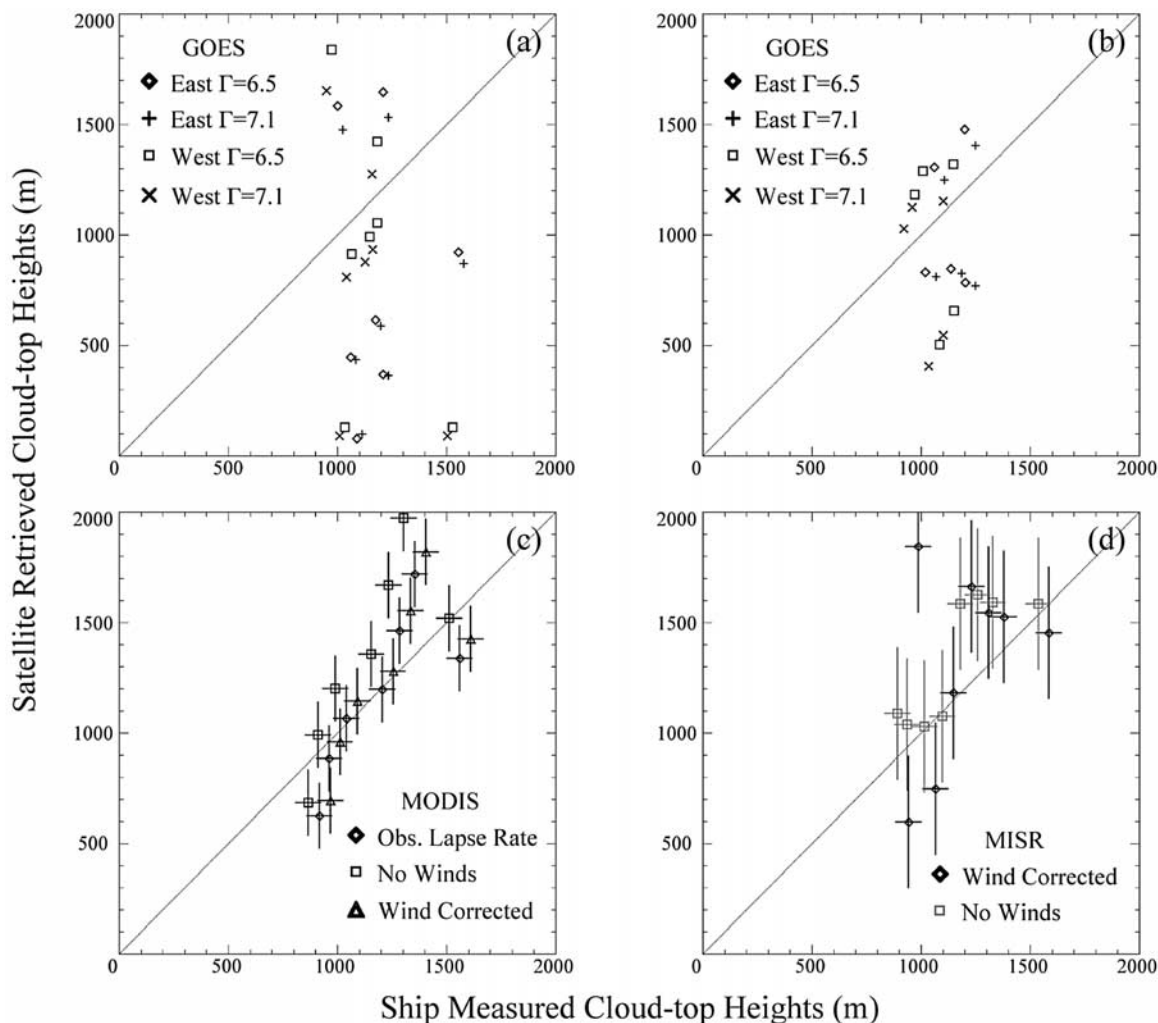


Figure 5. Same as Figure 2 but for retrievals using fixed atmospheric lapse rates. (a) ISCCP DX cloud top heights determined from fixed lapse rates of 6.5 and 7.1 °C km⁻¹ for GOES-East and GOES-West at 1500:00 UT. Retrievals using a lapse rate of 6.5 are shown as diamonds for GOES-East and squares for GOES-West. Retrievals using a lapse rate of 7.1 are indicated by pluses for GOES-East and crosses for GOES-West. Retrievals from each instrument are shifted slightly as an aid to interpretation. A one-to-one line is included for comparison. (b) Same as Figure 4a but for 1800:00 UT retrievals. (c) MODIS retrievals of cloud top height using fixed lapse rates. Diamonds indicate retrievals using the observed lapse rate, squares shown the results using the lapse rate derived using the MISR no winds retrievals, and triangles show results from the best wind retrievals. Error bars of ±150 m (±1 °C) are shown for the MODIS retrievals and ±60 m for the ship-based measurements. Points are shifted slightly as an aid to interpretation. (d) MISR stereo height retrievals coincident with the MODIS retrievals. Wind-corrected heights are shown as black diamonds, and no winds heights are shown as gray squares. Error bars of ±300 m are shown for the MISR retrievals and ±60 m for the ship-based measurements. Points are shifted slightly as an aid to interpretation.

ments reported in the MOD06 product, which are bilinearly interpolated SSTs taken from the GDAS model. Because satellite IR radiometers actually measure the temperature only within a few hundred microns of the surface [e.g., Donlon *et al.*, 2002], the comparison between the MODIS SST and the SST measured by the ship at 5 cm is appropriate. In most cases, the MODIS SST was within 0.5 °C of the ship-based measurements, with some evidence of a high bias, which would be expected given that the temperature falls with depth inside the water column. From the cloud top height measured by the ship-based instruments

and the cloud top temperature retrieved by MODIS values the lapse rate, Γ , in units of °C km⁻¹ can be calculated from

$$\Gamma = \frac{T_s - T_c}{h_c} \quad (1)$$

where T_s is the SST, T_c is the cloud top temperature, and h_c is the cloud top height. Note that the lapse rate calculated using equation (1) will be positive because the cloud top temperature will always be lower than the surface temperature.

Table 3. Statistical Comparison of ISCCP Retrievals and Associated Ship-Based Measurements for Constant Lapse Rate Retrievals

Observation	Mean (m)	σ (m)	RMS Error (m)	Correlation Coefficient r
Ship 1500 UT ($n = 7$)	1185	181		
GOES-East IR	2417	721	1409	0.03
GOES-East $\Gamma = 6.5$	809	608	692	0.04
GOES-East $\Gamma = 7.1$	740	556	696	0.04
GOES-West IR	2987	750	1978	-0.67
GOES-West $\Gamma = 6.5$	949	628	721	-0.51
GOES-West $\Gamma = 7.1$	869	575	708	-0.51
Ship 1800 UT ($n = 5$)	1157	61		
GOES-East IR	2721	357	1597	-0.06
GOES-East $\Gamma = 6.5$	1049	320	324	-0.27
GOES-East $\Gamma = 7.1$	961	292	343	-0.27
GOES-West IR	3075	553	1985	-0.23
GOES-West $\Gamma = 6.5$	1040	381	371	-0.14
GOES-West $\Gamma = 7.1$	952	349	384	-0.14

[37] Because three retrievals of the cloud top height are available that do not depend on the temperature structure of the atmosphere (ship-based, MISR no winds, MISR wind-corrected), it is possible to calculate three separate lapse rates. A mean “observational” lapse rate can be found using the ship-based measurements of T_s and h_c . Similarly, mean “no winds” and “wind-corrected” lapse rates can be found by using the MODIS SST as T_s and the MISR no winds and wind-corrected cloud top heights, respectively, as h_c . The MODIS cloud top temperature appears as T_c in all the calculations. The mean observational lapse rate for all seven cases was found to be $7.4^\circ\text{C km}^{-1}$, varying from 9.4 to $6.1^\circ\text{C km}^{-1}$ in specific cases. The no winds and wind-corrected lapse rates, derived from satellite retrievals alone, do not necessarily show very good agreement with the observational values on a case-by-case basis. Overall, however, the wind-corrected lapse rate was found to be $7.2^\circ\text{C km}^{-1}$, while the no winds lapse rate was $6.3^\circ\text{C km}^{-1}$. The close agreement between the mean observed and wind-corrected lapse rates with the $7.1^\circ\text{C km}^{-1}$ lapse rate determined by *Minnis et al.* [1992] for the California stratocumulus region is serendipitous, especially given the small sample size and large spread in the individual values.

[38] Figure 5c shows the cloud top heights calculated from the MODIS cloud top temperatures using the three lapse rates. Vertical error bars show the effect of a $\pm 1^\circ\text{C}$ error in the temperature retrieval, which corresponds to a height error of approximately ± 150 m. For comparison, Figure 5d shows the MISR retrievals from Figure 2d on the same scale as the other plots. Inspection of Figure 5c shows that the cloud top heights retrieved using the no winds lapse rate are biased high relative to the ship-based measurements. The wind-corrected and observational lapse rates differ from one another by only $0.2^\circ\text{C km}^{-1}$, so it is not surprising to find such good agreement between the cloud top heights retrieved using both lapse rates.

[39] Table 4 provides a statistical summary of the results obtained using the various lapse rates compared with the standard MISR and MODIS retrievals (reproduced from Table 2) for all cases where comparable MODIS data were available. It is immediately apparent that, just as was the

case with the ISCCP results, the MODIS cloud top heights derived using a constant lapse rate are all in significantly better agreement with the ship-based measurements than the MODIS cloud top heights derived from the cloud top pressures. The standard deviation and RMSE have both been significantly reduced, while the correlation coefficient has increased dramatically. In all cases, a linear fit of the MODIS cloud top heights to the ship-based measurements explains 64% of the variance, as determined by the R^2 value. Differences among the MODIS and MISR results are not statistically significant given the small sample size.

5. Conclusions and Recommendations for Future Work

[40] In an effort to better understand the performance characteristics of satellite cloud top height retrieval algorithms in marine stratocumulus regions, we have employed measurements of cloud top heights made by NOAA research vessels in the marine stratocumulus region off the western coast of South America during cruises in 2001, and 2003 to 2006. These observations were matched, spatially and temporally, with high-resolution retrievals from the MODIS and MISR instruments on the Terra satellite, as well as lower-resolution retrievals in the ISCCP DX data set.

[41] The ISCCP cloud top heights, determined from the cloud top pressures, were found to be biased high by between 1400 and 2000 m depending on the observation time and retrieval type. It was also found that employing a fixed atmospheric temperature lapse rate, such as $6.5^\circ\text{C km}^{-1}$ or $7.1^\circ\text{C km}^{-1}$, produced ISCCP cloud top height retrievals in significantly better agreement with the ship-based measurements. The specific lapse rate chosen had only a small effect on the results. However, the use of such a fixed lapse rate is likely to be appropriate only for low-level clouds. Moreover, the selection of an appropriate lapse rate may depend on the particular location [e.g., *Wood and Bretherton*, 2004; 2006]. The performance of the cloud top pressure approach applied globally to other cloud regimes was not assessed in this study.

[42] Similar to the ISCCP results, the MODIS cloud top heights derived from the cloud top pressures in the collection 5 MOD04 product were biased high by more than 2000 m relative to the ship-based measurements. The MISR standard retrievals, obtained from the F08_0017 version of the MISR L2TC product agreed with the ship-based measurements within 230 to 420 m on average. The large high bias in the MODIS retrievals was traced to the performance of the low-resolution GDAS model used to convert the observed cloud top temperatures to cloud top heights. The MISR cloud top heights, on the other hand, derived used a stereophotogrammetric method, do not require information about the atmospheric state and appear to provide a more legitimate comparison with climate models than the ISCCP or MODIS heights (derived from cloud top pressures), at least in the stratocumulus cloud region. These results highlight the importance of having independent satellite measurements of cloud top heights from MISR and MODIS to assess such potential issues, as suggested by *Ohring et al.* [2005]. Climatologies of cloud top heights from MISR data are available from the beginning of the Terra mission in 2000 to the present.

Table 4. Statistical Comparison of Ship-Based Measurements, MISR and MODIS Standard Retrievals, and MODIS Retrievals Using a Constant Lapse Rate

Observation	Mean (m)	σ (m)	RMS Error (m)	Correlation Coefficient r
Ship ($n = 7$)	1189	232		
MISR wind corrected	1314	474	420	0.41
MISR no winds	1388	292	245	0.85
MODIS pressure	2937	950	2004	-0.37
MODIS $\Gamma = 7.4$	1184	366	210	0.80
MODIS $\Gamma = 6.3$	1391	430	329	0.80
MODIS $\Gamma = 7.2$	1217	376	219	0.80

[43] As a way forward, these results also suggest two possible approaches for retrieving more accurate cloud top heights from MODIS and/or ISCCP in marine stratocumulus regions. The first approach would be to adopt a mean global lapse rate. The $7.1^{\circ}\text{C km}^{-1}$ lapse rate from *Minnis et al.* [1992] appears to work well in the stratocumulus regime examined in this study, but more work would be required to test its applicability in other regions. The MOD06 developers are presently testing several alternate methods for inversion situations appropriate for global application, including using a constant lapse rate. A second approach would use the MISR wind-corrected cloud top heights along with the MODIS or ISCCP SST and cloud top temperatures to establish a lapse rate climatology appropriate for marine stratocumulus regions. Because they are on the same satellite platform, it may also be possible to use the MISR and MODIS observations together to determine the exact regions where the MODIS retrievals have difficulty. When the MODIS cloud top pressure is determined using the IR algorithm in preference to the CO_2 -slicing approach, a comparison could be made with coincident retrievals from MISR on Terra. If the MISR heights are significantly lower, then it is likely an inversion condition exists. The MISR cloud top heights could then be used to determine an appropriate lapse rate for these regions. A similar methodology could be employed for use with the MODIS instrument on the Aqua satellite where lidar backscatter retrievals from CALIPSO could provide independent assessments of the actual height of the stratocumulus clouds, although with limited coverage relative to MISR.

[44] Marine stratocumulus clouds play an important role in the global climate system. While long-term data sets, such as ISCCP are valuable for understanding climatological trends, newer instruments including MISR and MODIS on the Terra satellite and MODIS and CALIPSO on the Aqua satellite should not be ignored. The instruments on Terra now provide a nearly continuous 8-year data set, with high spatial resolution. These data can be a valuable resource for understanding not only interannual variations in geophysical parameters like cloud top height, but differences in instrument and algorithm performance. With the amount of data available, more extensive studies employing more sophisticated statistical procedures should provide important new insights in the coming years.

[45] **Acknowledgments.** This research was performed at the Jet Propulsion Laboratory, California Institute of Technology, under a contract with the National Aeronautics and Space Administration. The MISR data were obtained from the NASA Langley Research Center Atmospheric Science Data Center. The MODIS data were obtained from the level 1

and Atmosphere Archive and Distribution System. Special thanks to Chris Fairall and his team at the NOAA Earth System Research Laboratory for conducting the field campaigns and making the data available to researchers. Thanks to Rich Frey, Space Science and Engineering Center, University of Wisconsin, for helpful comments as well as to two anonymous reviewers who provided useful comments that improved the clarity and readability of the manuscript. Thanks also to Dave Diner, Jet Propulsion Laboratory, California Institute of Technology, for supporting this work and providing valuable feedback, and Steve Klein, Lawrence Livermore National Laboratory, for initially suggesting this study.

References

- Ackerman, S. A., K. I. Strabala, W. P. Menzel, R. A. Frey, C. C. Moeller, and L. E. Gumley (1998), Discriminating clear sky from clouds with MODIS, *J. Geophys. Res.*, *103*(D24), 32,141–32,157, doi:10.1029/1998JD200032.
- Baum, B. A., and S. Platnick (2006), in *Introduction to MODIS cloud products, in Earth Science Satellite Remote Sensing, vol. 1, Science and Instruments*, edited by J. J. Qu et al., pp. 74–91, Springer, Berlin.
- Bony, S., and J.-L. Dufresne (2005), Marine boundary layer clouds at the heart of tropical cloud feedback uncertainties in climate models, *Geophys. Res. Lett.*, *32*, L20806, doi:10.1029/2005GL023851.
- Bretherton, C. S., T. Uttal, C. W. Fairall, S. E. Yuter, R. A. Weller, D. Baumgardner, K. Comstock, R. Wood, and G. B. Raga (2004), The EPIC 2001 stratocumulus study, *Bull. Am. Meteorol. Soc.*, *85*, 967–977, doi:10.1175/BAMS-85-7-967.
- Comstock, K. K., C. S. Bretherton, and S. E. Yuter (2005), Mesoscale variability and drizzle in southeast Pacific stratocumulus, *J. Atmos. Sci.*, *62*, 3792–3807, doi:10.1175/JAS3567.1.
- Davies, R., A. Horváth, C. Moroney, B. Zhang, and Y. Zhu (2007), Cloud motion vectors from MISR using sub-pixel enhancements, *Remote Sens. Environ.*, *107*, 194–199, doi:10.1016/j.rse.2006.09.023.
- Del Genio, A. D., A. B. Wolf, and M.-S. Yao (2005), Evaluation of regional cloud feedbacks using single-column models, *J. Geophys. Res.*, *110*, D15S13, doi:10.1029/2004JD005011.
- Derber, J. C., D. F. Parrish, and S. J. Lord (1991), The new global operational analysis system at the National Meteorological Center, *Weather Forecast.*, *6*, 538–547, doi:10.1175/1520-0434(1991)006<0538:TNGOAS>2.0.CO;2.
- Diner, D. J., et al. (1998), Multi-angle Imaging SpectroRadiometer (MISR) instrument description and experiment overview, *IEEE Trans. Geosci. Remote Sens.*, *36*, 1072–1087, doi:10.1109/36.700992.
- Donlon, C. J., P. J. Minnett, C. Gentemann, T. J. Nightingale, I. J. Barton, B. Ward, and M. J. Murray (2002), Toward improved validation of satellite sea surface skin temperature measurements for climate research, *J. Clim.*, *15*, 353–369, doi:10.1175/1520-0442[2002]015<0353:TIVOSS>2.0.CO;2.
- Fairall, C. W., A. B. White, J. B. Edson, and J. E. Hare (1997), Integrated shipboard measurements of the marine boundary layer, *J. Atmos. Oceanic Technol.*, *14*, 338–359, doi:10.1175/1520-0426(1997)014<0338:ISMOTM>2.0.CO;2.
- Fritz, S., and J. S. Winston (1962), Synoptic use of radiation measurements from satellite TIROS II, *Mon. Weather Rev.*, *90*, 1–9, doi:10.1175/1520-0493(1962)090<0001:SUORMF>2.0.CO;2.
- Genkova, I., G. Seiz, P. Zuidema, G. Zhao, and L. Di Girolamo (2007), Cloud top height comparisons for ASTER, MISR, and MODIS for trade wind cumuli, *Remote Sens. Environ.*, *107*, 211–222, doi:10.1016/j.rse.2006.07.021.
- Hartmann, D. L., M. E. Ockert-Bell, and M. L. Michelsen (1992), The effect of cloud type on earth's energy balance: Global analysis, *J. Clim.*, *5*, 1281–1304, doi:10.1175/1520-0442(1992)005<1281:TEOCTO>2.0.CO;2.
- Horváth, A., and R. Davies (2001a), Simultaneous retrieval of cloud motion and height from polar-orbiter multiangle measurements, *Geophys. Res. Lett.*, *28*, 2915–2918, doi:10.1029/2001GL012951.
- Horváth, A., and R. Davies (2001b), Feasibility and error analysis of cloud motion wind extraction from near-simultaneous multiangle MISR measurements, *J. Atmos. Oceanic Technol.*, *18*, 591–608, doi:10.1175/1520-0426(2001)018<0591:FAEAO>2.0.CO;2.
- King, M. D., W. P. Menzel, Y. J. Kaufman, D. Tanré, B.-C. Gao, S. Platnick, S. A. Ackerman, L. A. Remer, R. Pincus, and P. A. Hubanks (2003), Cloud and aerosol properties, precipitable water, and profiles of temperature and water vapor from MODIS, *IEEE Trans. Geosci. Remote Sens.*, *41*, 442–458, doi:10.1109/TGRS.2002.808226.
- Kollias, P., C. W. Fairall, P. Zuidema, J. Tomlinson, and G. A. Wick (2004), Observations of marine stratocumulus in SE Pacific during the PACS 2003 cruise, *Geophys. Res. Lett.*, *31*, L22110, doi:10.1029/2004GL020751.
- Large, W. G., and G. Danabasoglu (2006), Attribution and impacts of upper-ocean biases in CCSM3, *J. Clim.*, *19*, 2325–2346, doi:10.1175/JCLI3740.1.

- Menzel, W. P., and J. F. W. Purdom (1994), Introducing GOES-I: The first of a new generation of Geostationary Operational Environmental Satellites, *Bull. Am. Meteorol. Soc.*, *75*, 757–781, doi:10.1175/1520-0477(1994)075<0757:IGITFO>2.0.CO;2.
- Minnis, P., P. W. Heck, D. F. Young, C. W. Fairall, and J. B. Snider (1992), Stratocumulus cloud properties derived from simultaneous satellite and island-based instrumentation during FIRE, *J. Appl. Meteorol.*, *31*, 317–339, doi:10.1175/1520-0450(1992)031<0317:SCPDFS>2.0.CO;2.
- Mochizuki, T., T. Miyama, and T. Awaji (2007), A simple diagnostic calculation of marine stratocumulus cloud cover for use in general circulation models, *J. Geophys. Res.*, *112*, D06113, doi:10.1029/2006JD007223.
- Moroney, C., R. Davies, and J.-P. Muller (2002), Operational retrieval of cloud-top heights using MISR data, *IEEE Trans. Geosci. Remote Sens.*, *40*, 1532–1540, doi:10.1109/TGRS.2002.801150.
- Muller, J.-P., A. Mandanayake, C. Moroney, R. Davies, D. J. Diner, and S. Paradise (2002), MISR stereoscopic image matchers: Techniques and results, *IEEE Trans. Geosci. Remote Sens.*, *40*, 1547–1559, doi:10.1109/TGRS.2002.801160.
- Naud, C., J.-P. Muller, M. Haeffelin, Y. Morille, and A. Delaval (2004), Assessment of MISR and MODIS cloud top heights through intercomparison with a back-scattering lidar at SIRTa, *Geophys. Res. Lett.*, *31*, L04114, doi:10.1029/2003GL018976.
- Naud, C. M., B. A. Baum, M. Pavolonis, A. Heidinger, R. Frey, and H. Zhang (2007), Comparison of MISR and MODIS cloud-top heights in the presence of cloud overlap, *Remote Sens. Environ.*, *107*, 200–210, doi:10.1016/j.rse.2006.09.030.
- Ohring, G., B. Wielicki, R. Spencer, B. Emery, and R. Datta (2005), Satellite instrument calibration for measuring global climate change: Report of a workshop, *Bull. Am. Meteorol. Soc.*, *86*, 1303–1313.
- Platnick, S., M. D. King, S. A. Ackerman, W. P. Menzel, B. A. Baum, J. C. Riédi, and R. A. Frey (2003), The MODIS cloud products: Algorithms and examples from Terra, *IEEE Trans. Geosci. Remote Sens.*, *41*, 459–473, doi:10.1109/TGRS.2002.808301.
- Rossow, W. B., and R. A. Schiffer (1999), Advances in understanding clouds from ISCCP, *Bull. Am. Meteorol. Soc.*, *80*, 2261–2287, doi:10.1175/1520-0477(1999)080<2261:AIUCFI>2.0.CO;2.
- Rossow, W. B., A. W. Walker, D. E. Beusichel, and M. D. Roiter (1996), International Satellite Cloud Climatology Project (ISCCP) documentation of new cloud datasets, WMO/TD-737, 115 pp., World Meteorol. Org., Geneva, Switzerland. (Available online at http://pubs.giss.nasa.gov/abstracts/1996/Rossow_etal_1.html).
- Schmidt, G. A., et al. (2006), Present-day atmospheric simulations using GISS ModelE: Comparison to in situ, satellite, and reanalysis data, *J. Clim.*, *19*, 153–192, doi:10.1175/JCLI3612.1.
- Stephens, G. L. (2005), Cloud feedbacks in the climate system: A critical review, *J. Clim.*, *80*, 2261–2287.
- Stubenrauch, C. J., W. B. Rossow, F. Chérut, A. Chédin, and N. A. Scott (1999), Clouds as seen by satellite sounders (3I) and imagers (ISCCP). Part I: Evaluation of cloud parameters, *J. Clim.*, *12*, 2189–2213, doi:10.1175/1520-0442(1999)012<2189:CASBSS>2.0.CO;2.
- Tomlinson, J. M., R. Li, and D. R. Collins (2007), Physical and chemical properties of the aerosol within the southeastern Pacific marine boundary layer, *J. Geophys. Res.*, *112*, D12211, doi:10.1029/2006JD007771.
- Wang, J., W. B. Rossow, T. Uttal, and M. Rozendaal (1999), Variability of cloud vertical structure during ASTEX observed from a combination of rawinsonde, radar, ceilometer, and satellite, *Mon. Weather Rev.*, *127*, 2484–2502, doi:10.1175/1520-0493(1999)127<2484:VOCVSD>2.0.CO;2.
- Webb, M., C. Senior, S. Bony, and J.-J. Morcrette (2001), Combining ERBE and ISCCP data to assess clouds in the Hadley Centre, ECMWF and LMD atmospheric climate models, *Clim. Dyn.*, *17*, 905–922, doi:10.1007/s003820100157.
- Wood, R., and C. S. Bretherton (2004), Boundary layer depth, entrainment, and decoupling in the cloud-capped subtropical and tropical marine boundary layer, *J. Clim.*, *17*, 3576–3588, doi:10.1175/1520-0442(2004)017<3576:BLDEAD>2.0.CO;2.
- Wood, R., and C. S. Bretherton (2006), On the relationship between stratiform low cloud cover and lower-tropospheric stability, *J. Clim.*, *19*, 6425–6432, doi:10.1175/JCLI3988.1.
- Zhang, M. H., et al. (2005), Comparing clouds and their seasonal variations in 10 atmospheric general circulation models with satellite measurements, *J. Geophys. Res.*, *110*, D15S02, doi:10.1029/2004JD005021.
- Zong, J., R. Davies, J.-P. Muller, and D. J. Diner (2002), Photogrammetric retrieval of cloud advection and top height from the Multi-Angle Imaging SpectroRadiometer (MISR), *Photogramm. Eng. Remote Sens.*, *68*, 821–829.

S. P. de Szoeke, International Pacific Research Center, School of Ocean and Earth Science and Technology, Pacific Ocean Science and Technology Building, Room 401, 1680 East-West Road, University of Hawaii, Honolulu, HI 96822, USA.

M. J. Garay, Intelligence and Information Systems, Raytheon Corporation, 299 North Euclid Avenue, Suite 500, Pasadena, CA 91101, USA. (michael.j.garay@jpl.nasa.gov)

C. M. Moroney, Jet Propulsion Laboratory, California Institute of Technology, 4800 Oak Grove Drive, Pasadena, CA 91109, USA.